Atmospheric Research 147–148 (2014) 10–26

Contents lists available at ScienceDirect

Atmospheric Research

journal homepage: www.elsevier.com/locate/atmos

Sensitivity to Madden–Julian Oscillation variations on heavy precipitation over the contiguous United States

Charles Jones *, Leila M.V. Carvalho

Department of Geography, University of California, Santa Barbara, CA, USA
Earth Research Institute, University of California, Santa Barbara, CA, USA

ARTICLE INFO

Article history:
Received 10 October 2013
Received in revised form 30 April 2014
Accepted 2 May 2014
Available online 13 May 2014

Keywords:
Heavy precipitation
Madden–Julian Oscillation
Regional modeling

ABSTRACT

The Madden–Julian Oscillation (MJO) is the most prominent mode of tropical intraseasonal variability in the climate system and has worldwide influences on the occurrences and forecasts of heavy precipitation. This paper investigates the sensitivity of precipitation over the contiguous United States (CONUS) in a case study (boreal 2004–05 winter). Several major storms affected the western and eastern CONUS producing substantial economic and social impacts including loss of lives. The Weather Research and Forecasting (WRF) model is used to perform experiments to test the significance of the MJO amplitude. The control simulation uses the MJO amplitude observed by reanalysis, whereas the amplitude is modified in perturbation experiments. WRF realistically simulates the precipitation variability over the CONUS, although large biases occur over the Western and Midwest United States. Daily precipitation is aggregated in western, central and eastern sectors and the frequency distribution is analyzed. Increases in MJO amplitude produce moderate increases in the median and interquartile range and large and robust increases in extreme (90th and 95th percentiles) precipitation. The MJO amplitude clearly affects the transport of moisture from the tropical Pacific and Gulf of Mexico into North America providing moist rich air masses and the dynamical forcing that contributes to heavy precipitation.

1. Introduction

Heavy (or extreme) precipitation is among the most devastating weather phenomena because it is frequently accompanied by hazardous events such as lightning, hail, heavy snow, strong surface winds, and intense vertical wind shear. Heavy precipitation is also often associated with flash floods and landslides, which increase the potential for loss of life and property (e.g., Pielke and Downton, 2000). Even though heavy precipitation events occur infrequently, they have significant social and economic impacts (Changnon, 2003, 2011; Changnon et al., 2000; Easterling et al., 2000a,b; Long et al., 2012; Meehl et al., 2000). For instance, the United States National Weather Service registered an average of 76 flood-related fatalities per year during 2003–2012; for comparison the number of fatalities from lightning is 35 for the same period.

Significant efforts, therefore, have been dedicated to further understand the physical mechanisms associated with heavy precipitation and improve the forecast skill of synoptic situations that lead to such events (Houze, 2012; Kunkel et al., 2013; Lalaurette, 2003; Legg and Mylne, 2004; Palmer and Hagedorn, 2006; Tribbia, 1997; Zhu and Toth, 2001). In this context, it has been widely recognized that some types of climate modes, e.g. El Niño/Southern Oscillation (ENSO), North Atlantic Oscillation (NAO) and the Arctic Oscillation (AO), can significantly influence the occurrence of extreme events (Barry and Carleton, 2001; Gershunov, 1998; Gershunov and Barnett, 1998; Higgins et al., 2000b; Lavers and Villarini, 2013; Thompson and Wallace, 1998; Wettstein and Mearns, 2002).

* Corresponding author at: Department of Geography, University of California, Santa Barbara, CA 93106, USA.
E-mail address: cjones@eri.ucsb.edu (C. Jones).

http://dx.doi.org/10.1016/j.atmosres.2014.05.002

On subseasonal scales, the Madden–Julian Oscillation (MJO) is the most prominent mode of tropical intraseasonal variability in the climate system (Jones, 2009; Jones and Carvalho, 2006, 2011; Lau and Waliser, 2012; Madden and Julian, 1994; Pohl and Matthews, 2007; Zhang, 2013). The role of the MJO in affecting the occurrence of heavy precipitation on global and regional scales has been demonstrated (Donald et al., 2006; Jones et al., 2004b). Associations between the MJO and heavy precipitation have been found over Canada (Lin et al., 2010), the contiguous United States (Becker et al., 2011; Bond and Vecchi, 2003; Higgins et al., 2000b; Jones, 2000; Jones and Carvalho, 2012; Mo, 1999; Mo and Higgins, 1998a, 1998b; Ralph et al., 2011; Zhou et al., 2011), Mexico (Cavazos and Rivas, 2004; Mo and Higgins, 1998b), Caribbean (Martin and Schumacher, 2010), South America (Carvalho et al., 2002, 2004; De Souza and Ambrizzi, 2006; Gonzalez et al., 2008; Liebmann et al., 2004; Nogues-Paegle et al., 2000), Africa (Pohl and Camberlin, 2006a,b; Pohl et al., 2007), Australia (Wheeler et al., 2009), Asia (Barlow et al., 2005; Jeong et al., 2005, 2008; Zhang et al., 2009) and Indonesia (Hidayat and Kizu, 2010).

Since the life cycle of the MJO is longer than synoptic timescales, there is great interest in exploring the potential predictability associated with the MJO (Gottschalck et al., 2010; Hirons et al., 2013; Jones et al., 2004a,b; Vitart and Jung, 2010; Waliser et al., 2003; Weaver et al., 2011). Regarding the United States, several studies have shown evidence that the MJO influences the occurrence of heavy precipitation and forecast skill particularly in the boreal winter (Becker et al., 2011; Higgins et al., 2000b; Jones, 2000; Jones et al., 2011a,b; Zhou et al., 2012). In this process of further exploring the role of the MJO on extreme precipitation, many significant questions arise.

A complicating aspect is that the MJO exhibits a substantial degree of variability in terms of amplitude (or intensity), durations and phase evolution as it propagates eastward. Furthermore, the MJO shows significant irregularity such that MJOs can occur as single isolated events or in series of events in which successive episodes originate just after the termination of a previous event (Jones, 2009; Jones and Carvalho, 2011; Matthews, 2000, 2008). Moreover, the MJO displays large variations in amplitudes during its life cycle from event-to-event and may also interact with other modes of climate variability (e.g., ENSO, NAO and AO). This paper focuses especially on the amplitude of the MJO, which, as it is discussed next, is objectively defined by an index that aggregates anomalies in tropical convection and zonal circulation.

The objective of this study is to investigate the following question. *How sensitive is heavy precipitation over the contiguous United States to the amplitude of the MJO?* This is a complex problem that can be approached from many different angles. Here, we focus on a specific case study of heavy precipitation over the contiguous United States (CONUS) during the 2004–05 winter, when extremely wet conditions occurred over many areas in the Western and Midwest CONUS. While the MJO was active from mid-December until late January, its amplitude was close to the (median) climatological value. Therefore, we employ a regional numerical model to simulate the impact on precipitation of specific changes in the amplitudes of large-scale intraseasonal variability. It is important to note that other modes of variability (e.g., NAO, ENSO and PNA) are not filtered out from the sensitivity experiments. Thus, this study examines the joint sensitivity of MJO variations on precipitation, both as a single factor, as well as the result of its synergistic interactions with the aforementioned additional signals. This article is organized as follows. Section 2 describes the data sets and model. Section 3 discusses heavy precipitation and the MJO activity during the case study. Section 4 discusses the model setup and experiments. The impact of the MJO on the simulation of heavy precipitation is presented in Section 5. Section 6 presents the conclusions.

2. Data and model

Daily gridded precipitation from the NOAA Climate Prediction Center (CPC) unified gauge (CPC-uni) (Chen et al., 2008; Higgins et al., 2000a) is used to characterize precipitation during the extended winter season 1 Nov 2004–31 Mar 2005. The CPC-uni dataset uses an optimal interpolation technique to re-project precipitation reports to a grid with 0.25°-latitude by longitude; this dataset is one of the standard products used by CPC to evaluate the performance of reanalysis and Climate Forecast System (CFS) products (Higgins et al., 2008).

Daily averages of zonal wind components at 850-hPa (U850) and 200-hPa (U200) from the Climate Forecast System Reanalysis (CFSR) (Saha et al., 2010) and outgoing longwave radiation (OLR) (Liebmann and Smith, 1996) characterize large-scale circulation and tropical convective activity. Data from 1 January to 31 December 1979–2010 are used.

The same procedure discussed in Jones and Carvalho (2012) is employed to identify MJO activity. The seasonal cycle is first removed, and time series are detrended and filtered in frequency domain to retain intraseasonal variations (20–200 days) (Jones, 2009; Jones and Carvalho, 2011; Matthews, 2008). This procedure follows Matthews (2000, 2008) who determined that the wide 20–200 day band more accurately represents isolated MJO events; note that the filtering procedure is performed after removing the seasonal cycle.

MJO events are identified with combined empirical orthogonal function (EOF) analysis (Wilks, 2006) of equatorially averaged (15°S–15°N) U200 and U850 band-pass filtered anomalies. The first two EOFs and associated principal components (PCs) capture the MJO evolution; the first PCs (PC1, PC2) define the amplitude $(PC1^2 + PC2^2)^{0.5}$ and phase of the MJO. This procedure follows Wheeler and Hendon (2004) with the difference that our index is based on filtered data. A comparison between both indices indicated, as expected, much more noise in their index. Since the focus here is on a case study rather than a real-time application, we opted for the filtered index.

MJO events are defined when: 1) the phase angle between PC1 and PC2 systematically rotates counterclockwise, indicating eastward propagation at least to the Maritime Continent; 2) the normalized amplitude is always larger than 0.35; 3) the mean amplitude during the event is larger than 0.9; and 4) the entire duration of the event lasts between 30 and 90 days. Additional discussions for the definition of MJO events adopted here are in Jones (2009) and Jones and Carvalho (2011, 2012), whereas alternative definitions are found elsewhere (L'Heureux and Higgins, 2008).

The Weather Research and Forecasting (WRF version 3.5.1) model is used to investigate the sensitivity of heavy precipitation over the CONUS (Skamarock et al., 2008). WRF is the next generation, fully compressible, non-hydrostatic,

prognostic model suitable for idealized and realistic numerical simulations of the atmosphere. The model uses a terrain-following hydrostatic pressure coordinate in the vertical and the Arakawa-C staggering grid in the horizontal.

A large number of previous studies have employed WRF to investigate many distinct types of meteorological phenomena over the United States (Caldwell, 2010; Coleman et al., 2010; Ikeda et al., 2010; Jankov et al., 2009, 2011; Liu et al., 2011; Smith et al., 2010). The WRF configuration used in this study includes parameterizations for microphysics (vapor, ice, cloud, rain and snow) (Hong et al., 2004), transfer of solar and infrared radiation (i.e., rrtmg) (Iacono et al., 2008), Monin–Obukhov similarity theory (Skamarock et al., 2008), land-surface model (Unified Noah) (Chen and Dudhia, 2001), planetary boundary layer (YSU) (Hong et al., 2006) and cumulus convection (Kain–Fritsch) (Kain, 2004). The CFSR reanalysis are used as initial and boundary conditions for the WRF experiments. The choice of physical parameterizations used in this study is similar to the configuration employed in the real-time WRF forecasts over the CONUS produced by the National Center for Atmospheric Research (NCAR) (http://www.mmm.ucar.edu/wrf/users/forecasts.html). In addition, as will be discussed later, this choice of parameterizations has been used in other studies that have investigated the meteorological conditions during this case study.

3. Heavy precipitation and the MJO during November 2004–March 2005

The 2004–05 winter was characterized by extremely wet conditions over most of the Western and Midwestern CONUS. Fig. 1 (top) shows the total precipitation during 1 Nov 2004–31 Mar 2005 expressed as departure from climatology (1 Nov–31 Mar, 1948–2011). A large region from the Southwest to the Midwest received 150–250% above normal and several places in California, Nevada, Arizona, New Mexico and Texas registered 300–400% above normal. Furthermore, the precipitation during Jan 2005 contributed significantly to the winter season total (Fig. 1 bottom). In general, the wet conditions were associated with a blocking ridge in the Gulf of Alaska, an amplified trough over the southwestern CONUS and southward displaced jet stream and storm track. Several major storms contributed to heavy precipitation. The first storm produced 10–20 in. of snow in the Midwest (Ohio Valley) in 23 December, whereas heavy precipitation over California happened in 28–29 December. In particular, atmospheric rivers

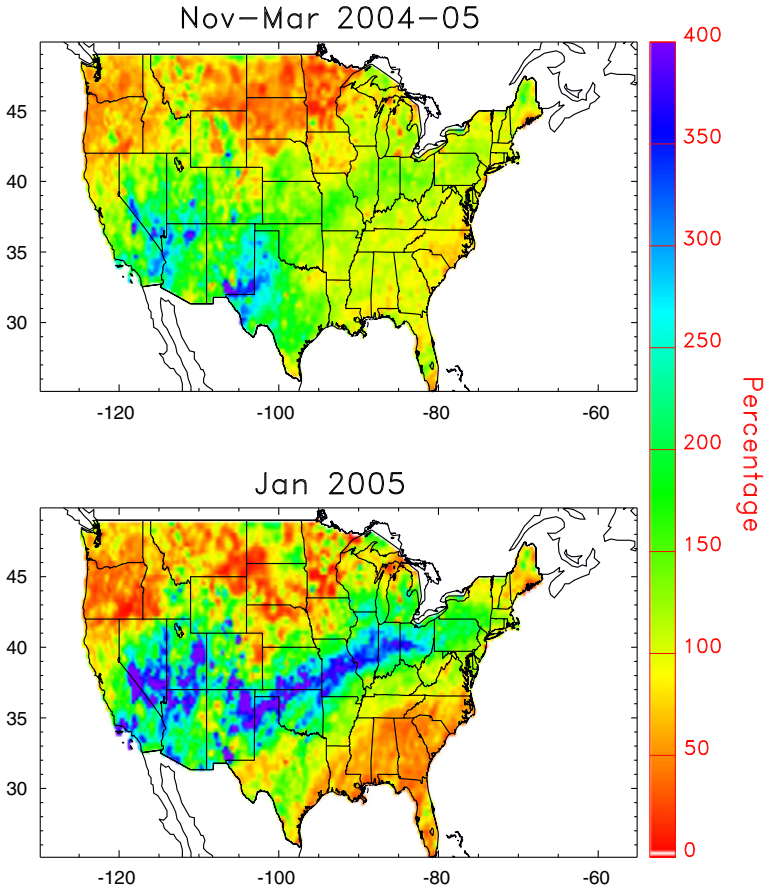

Fig. 1. (top) Total precipitation during 1 Nov 2004–31 Mar 2005 as departure from climatology; (bottom) departure from climatology of total precipitation during Jan 2005. Data: daily CPC-uni gridded precipitation 0.25-degrees lat/lon.

were very important during the 29–31 December precipitation events (Jankov et al., 2009, 2011; Smith et al., 2010). The third storm impacted the Midwest in 2–5 January. California was hit by heavy rainfall and snow in high elevations during 7–11 January, while the last major storm of the month contributed with heavy precipitation over the Midwest in 11–13 January.

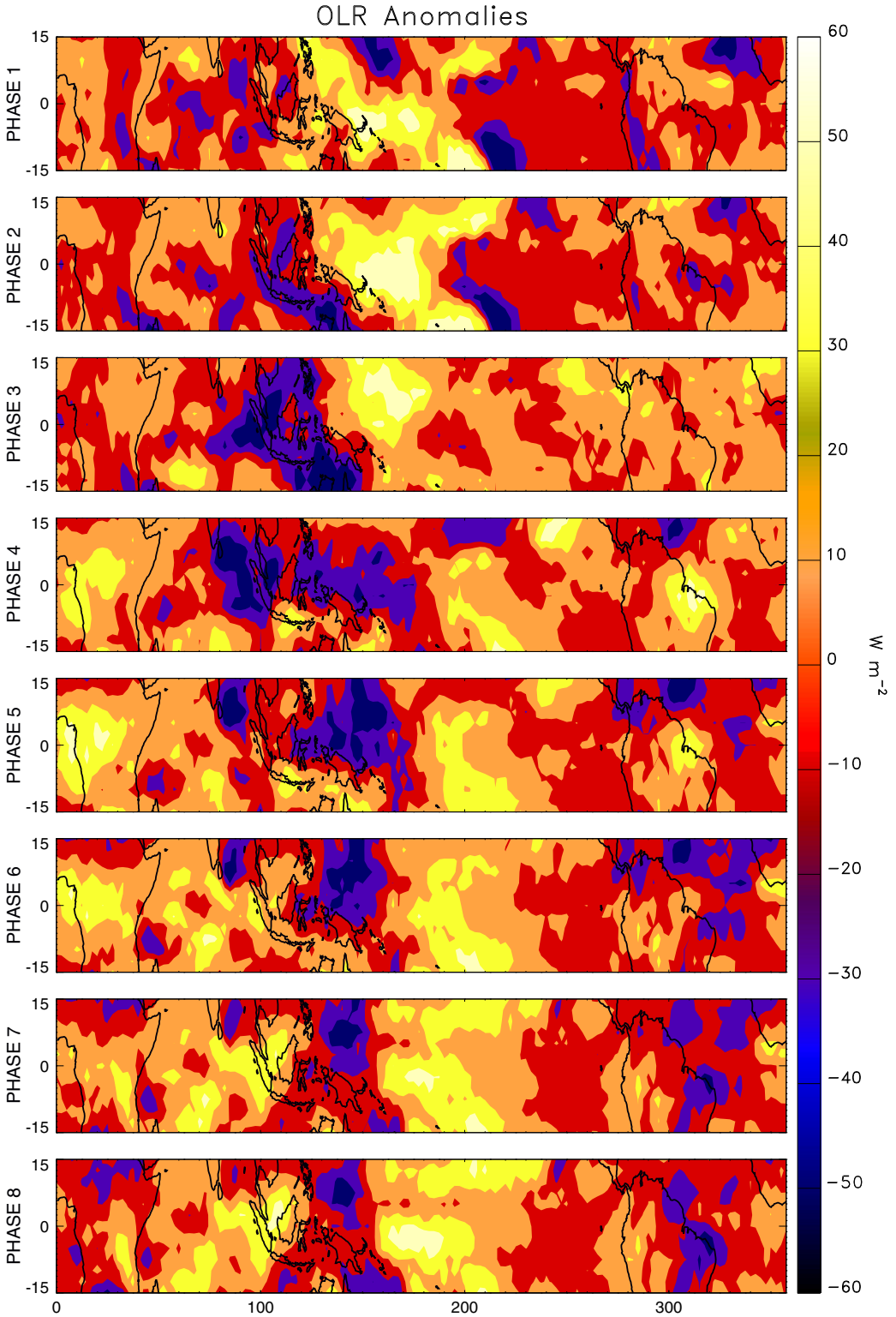

Fig. 2. Composites of bandpass-filtered OLR anomalies (W m^{-2}) during active MJO days (18 Dec 2004–20 Jan 2005).

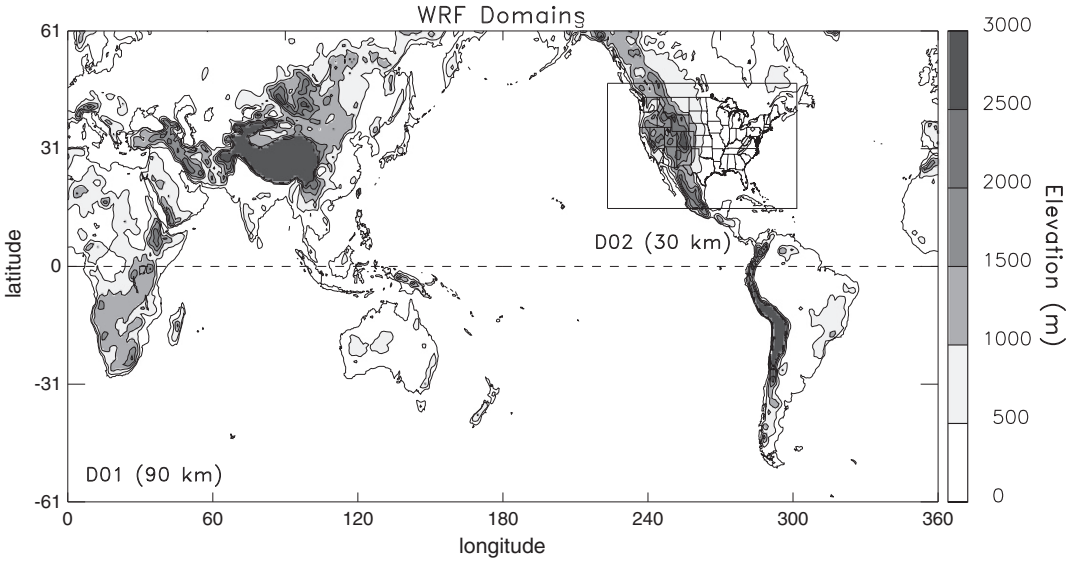

Fig. 3. Nested domains D01 (90 km) and D02 (30 km) of WRF model configuration. Shading indicates topography (m).

The impact of the storms was widespread and estimated in tens of millions of dollars and, more importantly, over 20 people were killed.[1]

The MJO was active during the 2004–05 winter season and contributed to the strength of the storms particularly in the Western CONUS. Fig. 2 shows the evolution of OLR anomalies averaged during the active MJO event (18 Dec 2004–20 Jan 2005). Enhanced tropical convective anomalies associated with the MJO developed over the Western Indian Ocean in 18 December (Phase 1) and propagated eastward in 19–24 December (Phase 2). Convective anomalies strengthened and continued to propagate eastward over Indonesia (Phase 3: 25 December–2 January; Phase 4: 3–8 January; Phase 5: 9–12 January). The MJO convection continued its movement into the western Pacific in 13–16 January (Phase 6), moved further east in 17–18 January (Phase 7) and finally ended in 19–20 January (Phase 8).

4. Model setup and experiments

In order to introduce the sensitivity experiments, we first discuss the model setup and biases in simulating precipitation over the CONUS during Nov–Mar 2004–05. WRF is used with two nested grids (Fig. 3) with 41 vertical levels; the top of the model is at 10-hPa. The large outer D01 domain (60S–60N; 0–360) has 90 km grid spacing and is designed to represent the MJO as well as capture its extratropical signals (Matthews et al., 2004; Seo and Son, 2012). The inner D02 domain with 30 km grid spacing covers the entire CONUS. Several experiments were performed to test the sensitivity of model configurations (e.g., domain sizes, vertical levels, time steps, and numerical stability). The most relevant to mention is the location of the lateral boundaries of the D02 domain, since their locations influence the evolution of synoptic systems coming from the west and tropical moisture fluxes entering the southern boundary. The present configuration showed the optimal balance among domain size, horizontal resolution, computational requirements and precipitation simulation skill. Lastly, it is worth mentioning that this study is part of an ongoing project to further understand the importance of the MJO on the predictability of extreme precipitation over the CONUS. While higher horizontal resolution would be desirable, this choice of grid spacings was based on computational requirements and a large set of ongoing predictability experiments.

In the control (CTRL) simulation, WRF is initialized on 1 November 2004 00UTC and run until 31 March 2005 18UTC. CFSR reanalysis is used for initial, lateral and lower boundary conditions (updated every 6 h). To ensure that the MJO signal is maintained throughout the simulation, grid nudging is applied in the D01 domain. Zonal and meridional components of the wind, temperature and specific humidity are nudged on all vertical levels towards the model interpolated CFSR reanalysis (nudging coefficient 0.0003 s^{-1}). Nudging is not applied on the D02 domain. Moreover, one-way nesting is used so that the model precipitation over the D02 domain is freely generated. Intraseasonal anomalies in OLR, U200 and U850 from the WRF simulation over the D01 domain compare very closely with the observed anomalies (e.g., Fig. 2) (not shown).

Fig. 4 shows the mean daily precipitation bias in WRF during 1 Nov 2004–31 Mar 2005. A wet model bias exceeding 6 mm day^{-1} is noted over the Western, Midwest and northeast CONUS, while the southeast has a dry bias of about −3 mm day^{-1}. The wet bias is particularly large over California, where the low horizontal model resolution is not able to properly resolve the Coastal Range and Sierra Nevada. Such wet bias is not uncommon in regional model simulations over the complex terrain in California. Smith et al. (2010), for instance, used an older WRF version (2.2) to examine the atmospheric river event during 29–31 December 2005 and reported large precipitation biases over the slopes of the Sierra Nevada, albeit using higher horizontal grid spacing (9 km). Likewise, Caldwell (2010) performed a comprehensive

[1] For details see: http://www.ncdc.noaa.gov/oa/climate/research/2004/california-storms2005.html.

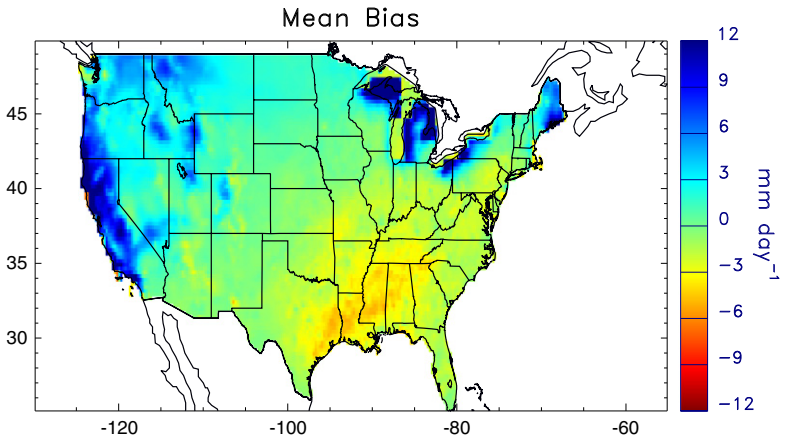

Fig. 4. Mean model bias (WRF minus CPC-uni) during 1 Nov 2004–31 Mar 2005 (mm day^{-1}).

comparison of regional and global climate model simulations of precipitation over California during winter and found that regional models tend to over predict precipitation on daily and interannual time scales.

We focus on the MJO event that occurred during 18 Dec 2004–20 Jan 2005 (Section 3). The mean daily precipitation estimated from CPC-uni and simulated by WRF during this period shows some consistent features (Fig. 5). To facilitate

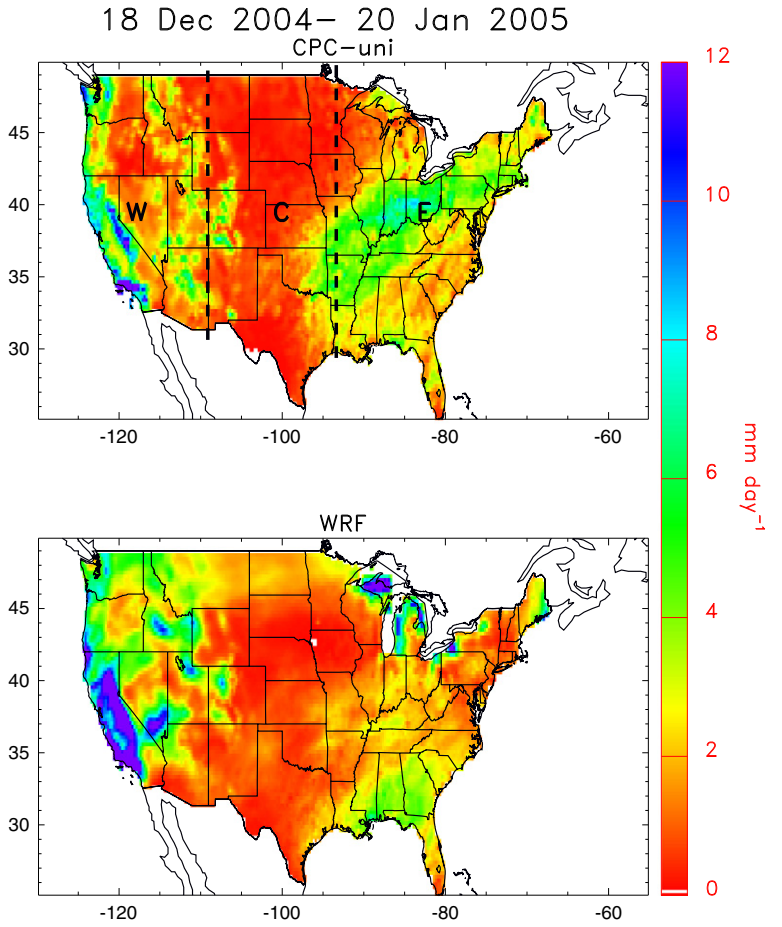

Fig. 5. (top) CPC-uni mean daily precipitation and (bottom) WRF mean daily precipitation (bias removed). Thick dashed longitudinal lines in top figure indicate western, central and eastern sectors over the contiguous United States. Period: 18 Nov 2004–20 Jan 2005.

the comparison, the mean model bias was removed from the WRF simulation. Precipitation over the Western CONUS is relatively well captured, although it is obvious that model precipitation is too heavy over California and, as previously mentioned, the coarse horizontal resolution does not resolve the spatial gradients in the coast, Central Valley and Sierra Nevada. The model also overpredicts precipitation over Oregon and Washington States, parts of Idaho and Nevada. The low precipitation amounts over the Central portion of the CONUS are relatively well simulated by WRF. Another deficiency is that the precipitation area from Oklahoma and Arkansas to the Northeast (Fig. 5 top) is not as high and is displaced further south in the model (Fig. 5 bottom). It is also interesting to note that the precipitation pattern over the eastern CONUS (Fig. 5 top) resembles the precipitation and storm track anomalies associated with the MJO (Becker et al., 2011), ENSO (Eichler and Higgins, 2006) and the Pacific North American (PNA) pattern (Grise et al., 2013). Possible interactions among these modes likely resulted in optimal conditions for the extremely wet 2004–05 winter season. In this context, that winter season was characterized by weak warm ENSO (tropical Pacific SST anomalies ~0.6C) and weak PNA (0.26 standardized index). The NAO, in contrast, was relatively strong (1.4 standardized index) in the same time period and may have contributed more significantly to heavy precipitation over the CONUS.

To get a better idea about the temporal variability, the daily precipitation is spatially averaged over three sectors. These sectors are arbitrarily defined but they separate the large precipitation in the western, small in the central and large in the eastern CONUS (Fig. 5 top). WRF realistically simulates the timing of the precipitation over the western sector (Fig. 6 top), although precipitation is still higher than the CPC-uni data even after removing the mean model bias. In contrast, more agreement is noted in the daily precipitation over the central sector (Fig. 6 middle). The first significant precipitation event is relatively well simulated by WRF over the eastern sector, whereas the model underestimates the second and has some difficulty in capturing the timing of the third event (Fig. 6 bottom). The mean biases (CPC-uni minus WRF), root-mean-square errors and correlations are respectively: -1.9 mm day^{-1}, 10.9 mm day^{-1}, 0.69 (Western), -0.09 mm day^{-1}, 0.53 mm day^{-1}, 0.66 (Central) and 0.64 mm day^{-1}, 3.71 mm day^{-1} and 0.40 (Eastern).

We now focus on the period when the MJO was active (18 Dec 2004–20 Jan 2005). To set the context for the importance of intraseasonal anomalies on the heavy precipitation over the CONUS, Fig. 7 shows the climatological frequency distribution of MJO amplitudes during the boreal winter (1 Nov–31 Mar, 1979–2010). The mean MJO amplitude was 1.34 during 18 Dec 2004–20 Jan 2005, therefore, below the climatological median value (1.67) indicating that it was not a remarkable MJO event in terms of amplitude.

Although the MJO is the most significant mode of tropical intraseasonal variability, it is important to mention that it is not the only source of intraseasonal variability in the atmosphere. To explore this aspect further, we consider the large-scale intraseasonal variability in the zonal component of the wind at 200-hPa (U200). We first apply a 20–100 day band-pass Murakami filter (Murakami, 1979) to the U200 time series (1 Nov 2004–31 Mar 2005). Next, a spatial filter is applied to retain only zonal wavenumbers 1–5. Fig. 8 shows the

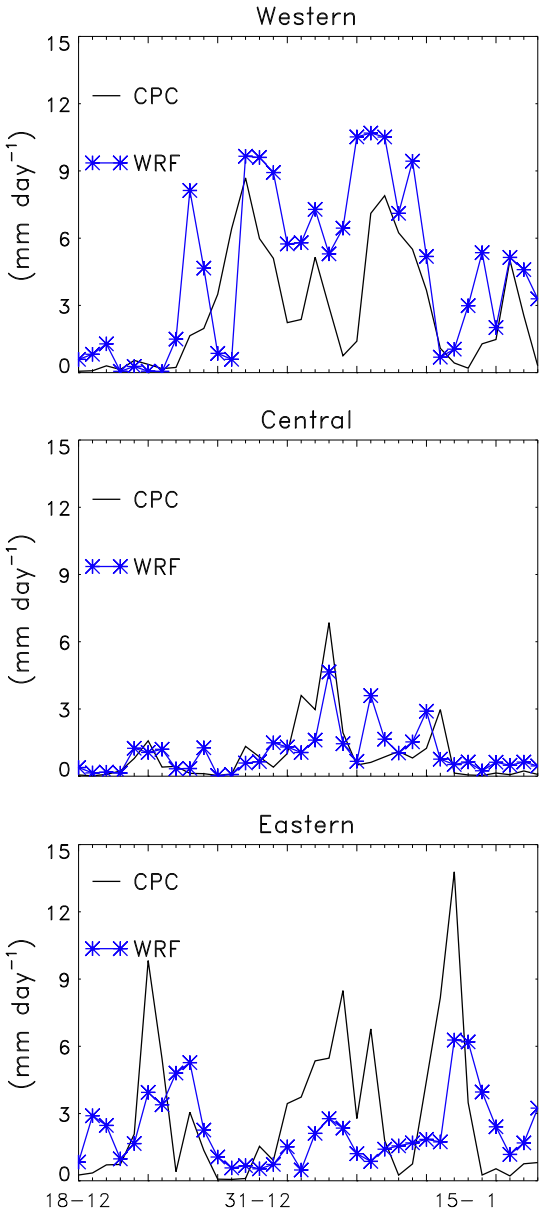

Fig. 6. Daily precipitation spatially averaged over the western (top), central (middle) and eastern (bottom) sectors of the contiguous United States. Black and blue curves are for CPC-uni and WRF precipitation; mean bias was removed from WRF precipitation. Period: 18 Nov 2004–20 Jan 2005.

standard deviations of anomalies from the seasonal cycle (top) and large-scale intraseasonal variations (bottom) during the case study (18 Dec 2004–20 Jan 2005). Over the tropical region, large-scale intraseasonal variations account for about 50–65% of the variance in U200; this is particularly the case over the Indian and western and eastern Pacific Oceans. It is also interesting to note that large-scale intraseasonal variability is especially large over the subtropical North Pacific and western North America (Fig. 8 bottom) accounting for almost 60% of the U200 variance. Since the MJO was active in this period, a significance portion of the U200 variability in these regions was

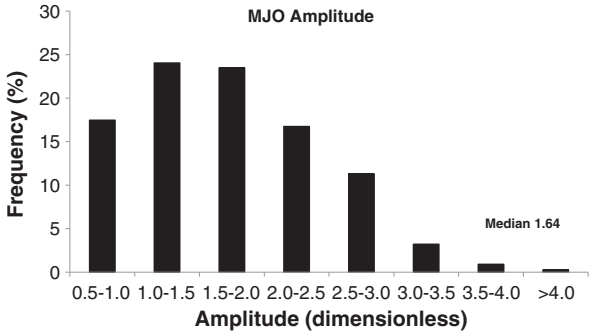

Fig. 7. Frequency distribution of MJO amplitudes during extended boreal winters (1 Nov–31 Mar, 1979–2010). Median value: 1.64.

associated with the eastward propagation of the MJO and interactions with the subtropical jet in the North Pacific via Rossby wave propagation (Matthews et al., 2004; Seo and Son, 2012). As mentioned previously, the NAO was also relatively strong during the case study and previous studies have shown that significant interactions between the MJO and NAO may occur (Cassou, 2008; Lin et al., 2009). Although we cannot rule out that intraseasonal variability in the NAO played a role in the heavy precipitation affecting the United States, our hypothesis is that the synoptic disturbances originated in the North Pacific were strongly influenced by the activity of the MJO during the case study.

To investigate the sensitivity of heavy precipitation over the CONUS to the amplitude of the MJO, a series of perturbation experiments are performed. WRF is initialized on 18 Dec 2004 00UTC and integrated until 20 Jan 2005. The model is nudged in D01 to a perturbed (interpolated) CFSR reanalysis with an altered large-scale intraseasonal signal. The signal is defined here in the following way. First, a 20–100 day band-pass Murakami filter (Murakami, 1979) is applied to the time series of geopotential height, temperature, zonal, meridional wind components and specific humidity (all model levels). The application of the recursive Murakami filter is necessary because of the short length of the time series. Next, a spatial filter is applied to these variables by retaining only zonal wavenumbers 1–5 which is typical of the large-scale nature of the MJO (Hendon and Salby, 1994; Jones, 2009).

A total of 7 perturbation experiments are performed. In the NOMJO experiment, WRF is nudged in D01 to interpolated CFSR reanalysis in which the MJO signal is removed. In the other experiments, the observed MJO signal is modified to different amplitudes: reduced to 25% and 50% and increased by 25%, 50% and 75%. The modification of the

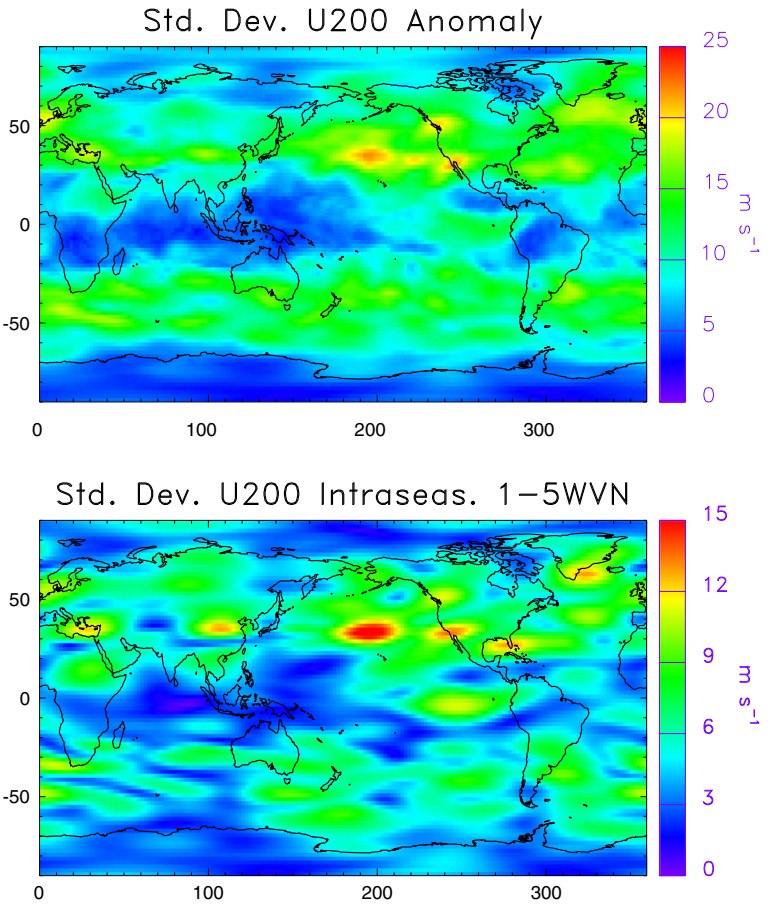

Fig. 8. Standard deviations of the zonal component of the wind at 200 h-Pa (U200) anomalies from the seasonal cycle (top) and large-scale intraseasonal anomalies (bottom).

MJO signal is done for each day during 18 Dec 2004–20 Jan 2005, grid point in D01, variable and model level. Moreover, we emphasize that nudging is not applied in D02 and WRF is run with one-way nesting.

To illustrate the procedure above, Fig. 9 shows the U200 field during 9 Jan 2005 when heavy precipitation impacted the western coast of the United States. The perturbed U200 can be written as: $U200_{Pert} = U200 + A \times U200_{LGIS}$ where U200 is the original field, A = [−1, −0.75, −0.50, 0, 1.25, 1.50, 1.75] the perturbation intensities and $U200_{LGIS}$ is the large-scale intraseasonal signal calculated as above (A = 0 for the control experiment). Fig. 10 shows U200 along zonal sections over the subtropical North Pacific (top) and equator (bottom); each curve shows $U200_{Pert}$ for different values of A. Note that the procedure modifies variations between 20 and 100 days and zonal wavenumbers 1–5 (the large-scale intraseasonal signal has zero mean). Variations outside these bands are not modified and therefore any other possible signals associated with ENSO, PNA and NAO are still retained including synergistic interactions among the MJO and these other modes of variability. In addition, note that WRF is nudged in D01 towards $U200_{Pert}$ (i.e., the total field and not only to the large-scale intraseasonal signal).

In summary, these experiments are designed so that WRF is nudged to the interpolated CFSR reanalysis in D01 with observed (CTRL) or modified large-scale intraseasonal signals (perturbations). The influence of the MJO on the precipitation over the CONUS is hence done through the lateral boundaries of D02 (especially the western boundary) and only large-scale intraseasonal signals are modified. Similar methods have been successfully used in regional model experiments. For instance, Gustafson and Weare (2004) employed the Mesoscale Model version 5 (MM5) over the Indian and western Pacific Oceans to investigate the initiation of the MJO. The control case forced with reanalysis was compared against perturbation experiments in which 30–70 day signals from the reanalysis were filtered out from the lateral boundary conditions.

To help understand more details about the WRF experiments, Table 1 shows observed values and perturbations in MJO amplitude. In the CTRL experiment (dashed lines central column), the observed mean amplitudes of the MJO were 1.67 (7–11 Jan), 1.30 (9–13 Jan) and 1.08 (11–15 Jan). Notice that during the heavy precipitation event that hit the western CONUS on 07–11 Jan 2005, the mean MJO amplitude was very close to the climatological median value (1.64). As the storms moved further east over the central (9–13 Jan) and eastern (11–15 Jan) CONUS, the MJO weakened and the mean amplitudes were near the lower quartile of the climatological winter frequency distribution (Fig. 7). The other columns in Table 1 show the changes in the MJO signal for each perturbation experiment from NOMJO (left) up to 75% increase (right); rows indicate the mean MJO amplitudes and corresponding percentiles. The perturbation experiments for the storms during 7–11 Jan cover a wide range of MJO amplitudes from NOMJO signal up to amplitudes in the 95th percentile (top row). Because the MJO weakened as it propagated eastward, the perturbation experiments cover different ranges of the frequency distribution for the storms over the central (middle row) and eastern (bottom row) CONUS.

5. Variations in the MJO and heavy precipitation over the CONUS

The following analysis is performed to investigate the importance of MJO amplitudes in controlling the distribution of precipitation across the CONUS. We focus on the period 18 Dec 2004–20 Jan 2005 when the MJO event evolved (e.g., Fig. 2). The sensitivity of heavy precipitation to the amplitude of large-scale intraseasonal signals is investigated by aggregating the daily precipitation over the western, central and eastern CONUS sectors (see Fig. 5).

Fig. 11 shows the frequency distribution of precipitation aggregated over the three sectors. The plot is constructed by taking precipitation time series ($P > 0.01$ mm day^{-1}) from all grid points in each sector and calculating statistics (interquartile range, median, 90th and 95th percentiles). For convenience, the plot shows statistics from CPC-uni data and WRF CTRL experiment. Since WRF exhibits a wet bias over the western CONUS, precipitation from WRF has a wider frequency distribution and heavier precipitation than CPC-uni. More agreement is noted over the central CONUS, although extreme precipitation values are smaller in the WRF CTRL experiment than in CPC-uni. Given the dry model bias in the eastern CONUS, the interquartile range is wider in the CPC-uni data than in WRF CTRL; 90th

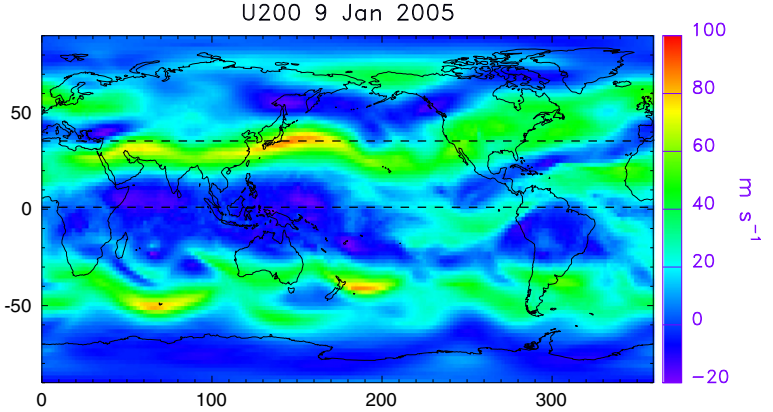

Fig. 9. Zonal winds at 200 h-Pa (U200) on 9 January 2005. Dashed lines indicate zonal sections shown in Fig. 10.

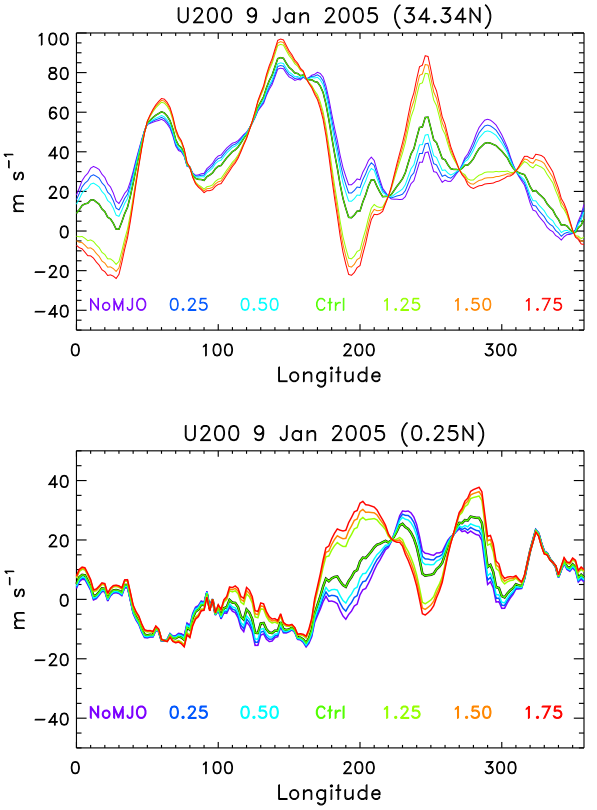

Fig. 10. Zonal winds at 200 h-Pa (U200) along 34.34 N (top) and 0.25 N (bottom). Curves show U200 with different MJO signals: (NoMJO), reduced to 0.25, 0.5, and control (CTRL), increased by 0.25, 0.5 and 0.75 (see text for additional details).

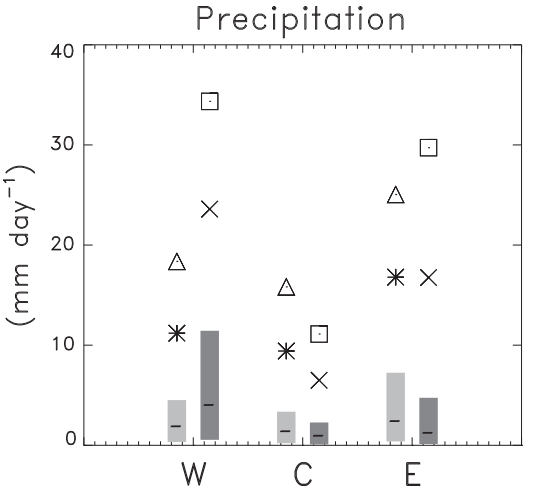

Fig. 11. Frequency distributions of precipitation aggregated over the (W) western (C), central and (E) eastern CONUS sectors. Statistics are computed by taking precipitation time series ($P > 0.01$ mm day^{-1}) from all grid points in each sector. CPC-uni: interquartile range (light shaded box), median value (tick), 90th (star) and 95th (triangle) percentiles; WRF-CTRL: interquartile range (dark shaded box), median value (tick), 90th (X) and 95th (square) percentiles. Period: 18 Dec 2004–20 Jan 2005.

percentile from WRF CTRL is consistent with CPC-uni. These statistics are used for comparison with the WRF sensitivity experiments.

Fig. 12 shows sensitivity plots for each CONUS sector and WRF experiment; the statistics are calculated as described above. The horizontal axis indicates that the WRF experiment from the NOMJO case to the MJO signal is being increased by 75%. In the western sector (Fig. 12 top), the CTRL experiment shows median precipitation of about 3.5 mm day^{-1}, interquartile range of 0.5–12 mm day^{-1} and 90th and 95th percentiles of 24 mm day^{-1} and 34 mm day^{-1}, respectively. It is interesting to note that as the MJO signal increases from NOMJO to 75% increase, the median and lower quartiles show moderate increases. In contrast, there is an almost linear and significant increase in the upper quartile and extreme values (i.e., 90th and 95th percentiles) as the MJO signal changes from NOMJO to CTRL experiments. As the MJO signal is increased in the 1.25–1.75 experiments, the upper quartile and extreme values show further increases suggesting a non-linear rate of changes. A somewhat similar behavior is seen for the statistics in the central sector (Fig. 12 middle) (note that precipitation scales are different for each sector) indicating nearly linear increases with MJO signal. Over the eastern sector (Fig. 12 bottom), the interquartile range responds differently with increases in MJO amplitudes compared to other sectors; only the extremes (90th and 95th

Table 1
MJO amplitudes. Central column (dashed lines) indicates observed values (bold) during three periods and respective percentiles of the climatological frequency distribution of MJO amplitudes during winter (1 Nov–31 Mar, 1979–2010). Other columns show changes in MJO signal for each perturbation experiment from NOMJO (left) up to 75% increase (right); rows indicate the mean MJO amplitudes and corresponding percentiles during the WRF case study. See text for additional explanation.

	MJO amplitude						
			07-11 Jan 05				
Mean	0	0.42	0.84	1.67	2.09	2.51	2.93
percentile	N/A	9th	19th	median	72th	84th	95th
			9-13 Jan 05				
Mean	0	0.33	0.65	1.3	1.63	2	2.28
percentile	N/A	7th	15th	29th	~median	69th	78th
			11-15 Jan 05				
Mean	0	0.27	0.54	1.08	1.35	1.62	1.89
percentile	N/A	6th	12th	24th	46th	~median	65th
Change in MJO amplitude	Removed	Decreased to 25%	Decreased to 50%	CTRL	Increased by 25%	Increased by 50%	Increased by 75%

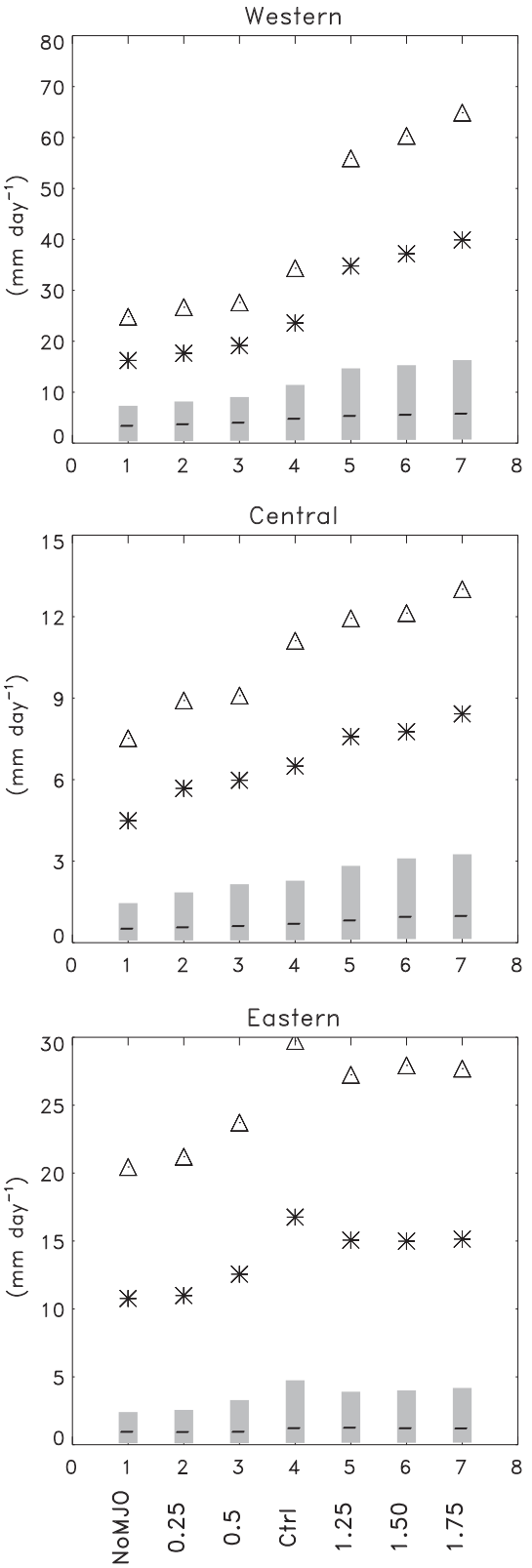

percentiles) in precipitation appear to have a linear relationship with the MJO signal. Lastly, the model performance can be evaluated comparing Fig. 11 and the statistics for the CTRL run in Fig. 12. Since the mean model bias has not been removed in these calculations, precipitation statistics in the western sector are higher in WRF (Fig. 12 top) than in the CPC-uni data; the same happens to some extent in the central sector. Conversely, due to the dry model bias in the eastern sector, statistics for WRF are lower than in the CPC-uni data.

The results above show that the MJO had a pronounced influence on the precipitation over the CONUS, particularly on extreme events. In order to shed some light on the changes in the atmosphere, Fig. 13 shows the synoptic conditions during the heavy precipitation in the western (left column) and eastern (right column) sectors. In 9 January, a low surface pressure system and a trough in the 500-hPa geopotential height (Fig. 13a) were situated over the Pacific Northwest, whereas intense southwesterly flow brought significant amounts of tropical moisture especially over California and northern Mexico (Fig. 13c). It is especially interesting to note that the moist atmospheric flow runs nearly perpendicular to the main topographic barriers in California, thus explaining the strong uplift and heavy precipitation. In 13 January, the heavy precipitation on the Midwest was associated with the low surface pressure and 500-hPa trough over the northern-central parts of North America (Fig. 13b). Intense moisture flux is carried from the Gulf of Mexico towards the eastern CONUS (Fig. 13d).

Fig. 14 shows differences in geopotential height (500-hPa) between the CTRL and perturbation experiments during 9 Jan (left) and 13 Jan 2005 (right). The top row indicates the NOMJO minus CTRL experiment, whereas the middle and bottom rows show differences between MJO signal decreased by 25% minus CTRL and MJO increased by 75% minus CTRL, respectively. Removing the MJO signal significantly weakens the trough by more than 300 m over the Pacific Northwest on 9 Jan 05, when the storms hit the western CONUS (Fig. 14a). As the MJO signal is decreased by 25% (Fig. 14b) and increased by 75% (Fig. 14c), the trough over the Pacific Northwest strengthens, but note that the relationship is not linear. Changing the MJO signal affects the magnitude of the 500-Pa geopotential height when the storms hit the Midwest as well (Fig. 14-d–f).

The sensitivity of vertically integrated moisture flux for each WRF experiment is constructed as previously explained. Over the western sector (Fig. 15 top), the MJO signal shows significant modulation on the moisture flux statistics with notable impacts in the upper tails of the frequency distributions. The importance of the MJO in controlling changes in moisture flux is also noted over the central and eastern sectors (Fig. 15 middle and bottom).

Moisture of tropical origin is important for the winter storms affecting North America. In particular, the moisture rich patterns known as "atmospheric rivers" can bring considerable amounts

Fig. 12. Sensitivity of daily precipitation (mm day^{-1}) over the western (top), central (middle) and eastern (bottom) sectors of the contiguous United States. Plots are for sensitivity experiments with different MJO signals (horizontal axis): NoMJO, reduced to 0.25, 0.5, control (CTRL), increased by 0.25, 0.5 and 0.75. Shaded boxes indicate interquartile range, median value (tick), 90th (star) and 95th (triangle) percentiles. Statistics are calculated from all grid points in each sector. Period: 18 Dec 2004–20 Jan 2005.

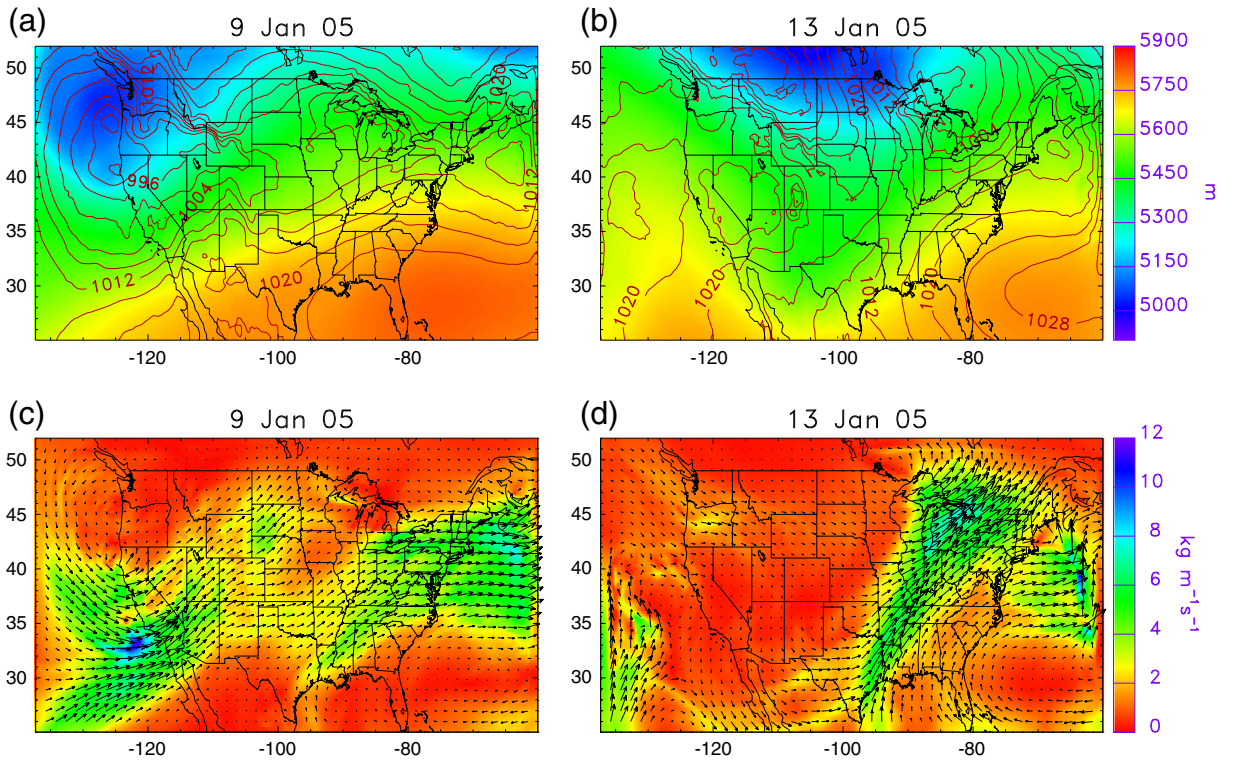

Fig. 13. Synoptic conditions during winter storms in the western (left) and eastern (right) United States. Top row shows geopotential height at 500-hPa (shading) and sea level pressure (contours) with 4-hPa interval. Bottom row shows vertically integrated moisture flux intensity (shading) and vectors the zonal and meridional components of the vertically integrated moisture flux. Fields are from WRF control simulation.

of tropical water vapor into the subtropics and midlatitudes providing the perfect conditions for heavy precipitation (Coleman et al., 2010; Kim et al., 2013; Kingsmill et al., 2013; Ralph and Dettinger, 2012; Rutz and Steenburgh, 2012; Smith et al., 2010). The MJO has been shown to control the timing of atmospheric rivers and the intensity of snow-water equivalent over the Sierra Nevada (Guan et al., 2012). These results above indicate that the large-scale atmospheric circulation patterns associated with the MJO contributed substantially to the tropical moisture transport into the CONUS and, therefore, on the heavy precipitation events during 18 Dec 2004–20 Jan 2005.

The importance of the MJO signal is also investigated on two dynamical terms. Fig. 16 shows the sensitivity of positive absolute vorticity advection at 500-hPa for each WRF experiment. In the western sector, the interquartile range and 90th and 95th percentiles increase as the MJO signal increases from NOMJO to CTRL experiments (Fig. 16 top). There appears to be a more pronounced increase from CTRL to 1.25 experiment and then a more slow increase to 1.50 and 1.75 experiments. The impact of the MJO signal on the extreme values is much more distinct than on the median or lower quartile. Somewhat similar changes are noted over the central and eastern sectors but scaled a little different. The sensitivity of positive temperature advection at 500-hPa (Fig. 17) for each WRF experiment is remarkably similar to the changes in positive 500-hPa vorticity advection over the three CONUS sectors.

6. Summary and conclusions

The MJO is the most important mode of tropical intraseasonal variability with a key role in bridging weather and climate variability. Although the MJO has been the focus of intense research, several key aspects need to be further understood. The main goal of this paper is to determine the extent to which the amplitude of the MJO modifies weather systems and the statistical properties of precipitation over the CONUS particularly in heavy events. This question is investigated with sensitivity experiments using the WRF model and focusing on a case study. The 2004–05 winter season was characterized by abnormally wet conditions over a large region from the southwest to the Midwest United States. Heavy precipitation events during the season had major social and economic impacts including the loss of lives.

CFSR reanalysis is used as initial, lateral and lower boundary conditions for a control simulation for the period 1 Nov 2004–31 Mar 2005. WRF is capable to realistically simulate the precipitation variability over the CONUS, although large biases occur over the Western and Midwest United States. The relatively coarse (30 km) grid spacing in the domain covering the CONUS is likely responsible for some of the biases over the complex topography in California. Undoubtedly, the choice of physical parameterizations can have significant impacts in the model simulated precipitation as discussed in Jankov et al. (2009, 2011). Although the combination of physical parameterizations employed in this study has been extensively used in the

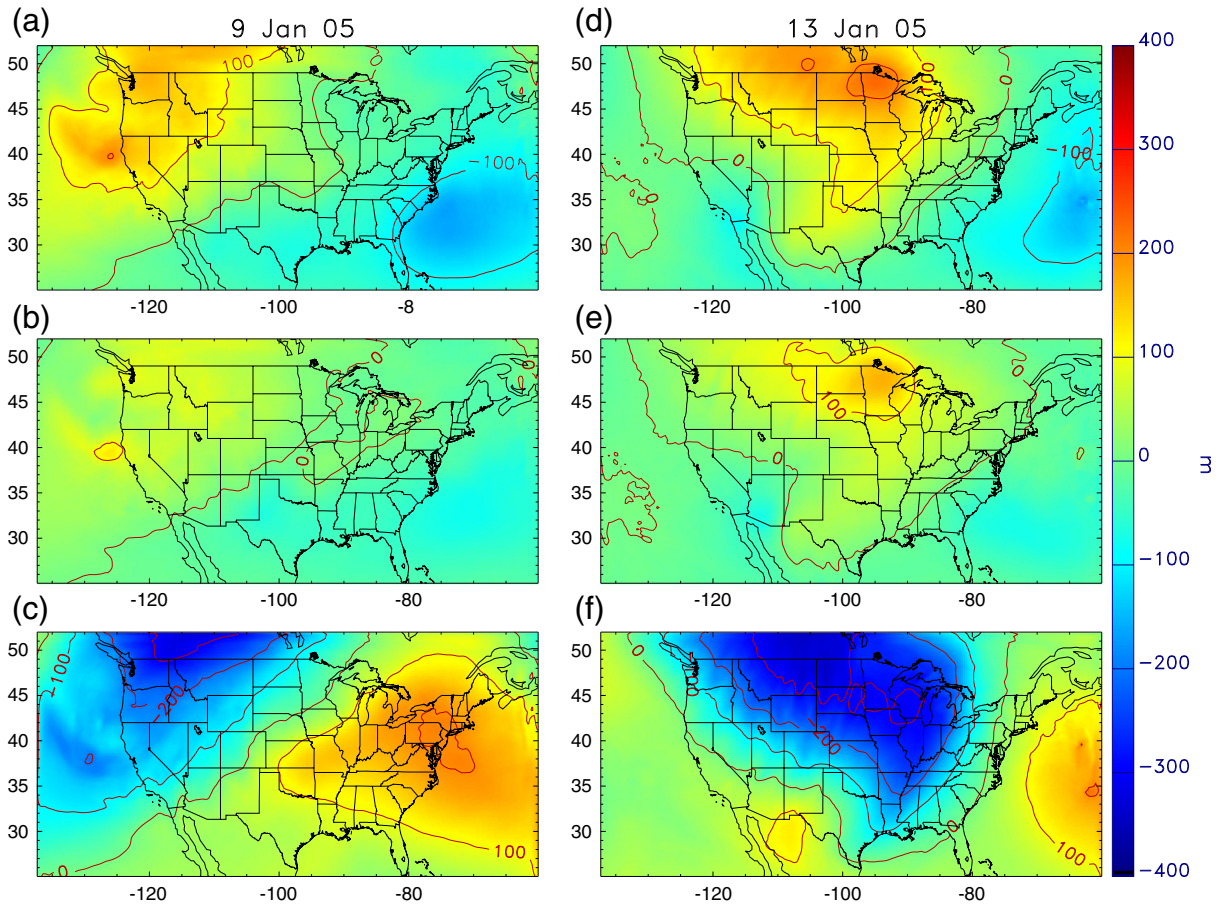

Fig. 14. Synoptic conditions during winter storms in the western (left: 9 Jan 2005) and eastern (right: 13 Jan 2005) United States. Rows show differences in geopotential height at 500-hPa: NOMJO minus CTRL (Top), MJO decreased by 25% minus CTRL (Middle) and MJO increased by 75% minus CTRL (bottom). Contour interval: 100 m.

WRF modeling community (e.g., real-time forecasts at NCAR), additional research is needed to improve model precipitation skill particularly over complex terrain.

WRF experiments are performed to test the hypothesis that the amplitude of the MJO plays an important role in the precipitation especially in the synoptic systems forming in the north Pacific and extreme precipitation over the CONUS. Sensitivity experiments are designed such that the large-scale intraseasonal signal in the atmospheric fields in the outer domain is decreased or increased. Grid nudging is applied only in the outer domain and the influence of the MJO is done through the lateral boundaries of the inner domain over the CONUS.

Daily precipitation is aggregated in western, central and eastern sectors over the CONUS and the frequency distribution is analyzed for each sensitivity experiment. The amplitude of the MJO has clear influences on the precipitation statistics especially in the median and interquartile range over the western and central CONUS. Furthermore, increases in MJO amplitude are strongly related to increases in extreme (90th and 95th percentiles) values of precipitation over all sectors. Additionally, the MJO amplitude clearly affects the transport of moisture from the tropical Pacific and Gulf of Mexico into North America providing moist rich air masses. Nearly linear relationships are found between increases in the amplitude of the MJO and increases in vertically integrated moisture flux. Along with moisture supply, the amplitude of the MJO is an important factor in modulating the dynamical forcing in the mid-troposphere and contributing to heavy precipitation over the CONUS.

The case study discussed here investigated the importance of the MJO amplitude on the precipitation over the CONUS. It is important to note, however, that the MJO is not the only source of intraseasonal variability and other climate modes have important influences on the synoptic systems producing precipitation over the CONUS. The case study analyzed here was characterized by weak warm ENSO and PNA patterns and moderate positive NAO phase. The sensitivity experiments carried out in this study, however, modified only the amplitudes of large-scale intraseasonal variability; signals associated with ENSO, NAO and PNA were not filtered out. Because of this, the results presented here examined the joint sensitivity of MJO variations on precipitation, both as a single factor, as well as the result of its synergistic interactions with other modes of variability. Other model experiment techniques such as factor separation (Stein and Alpert, 1993) can be applied to isolate the impact of single signals. Further elucidating the interactions among these climate modes, including the

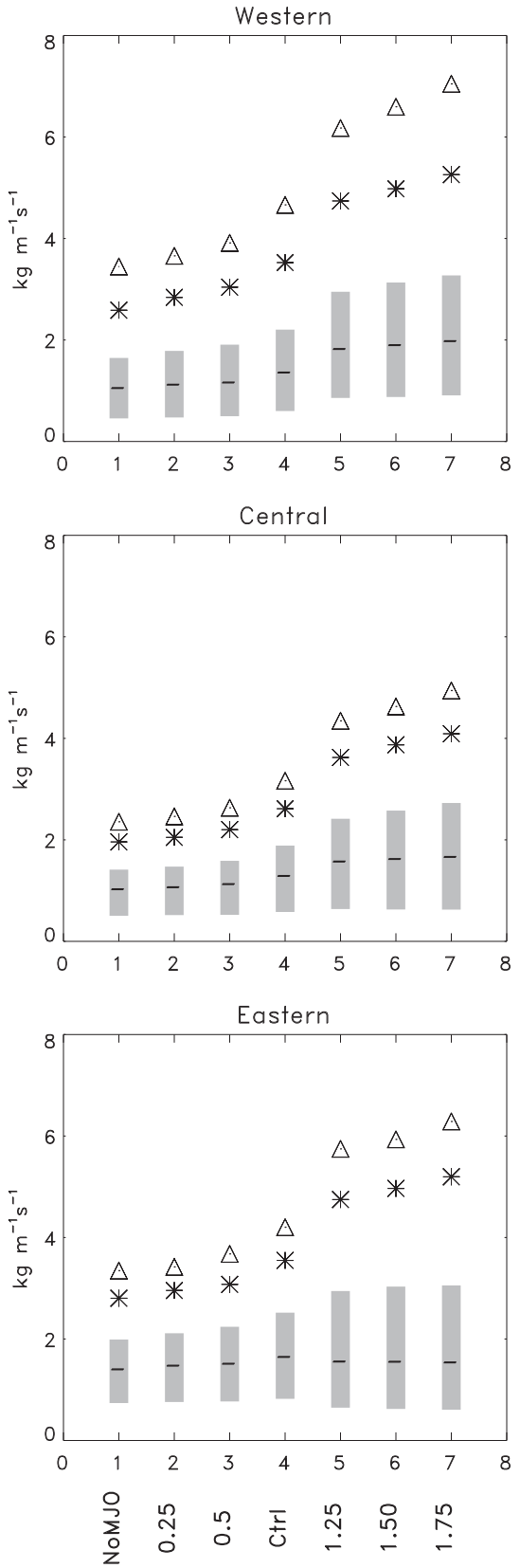

Fig. 15. As in Fig. 12 but for sensitivity of vertically integrated moisture flux intensity.

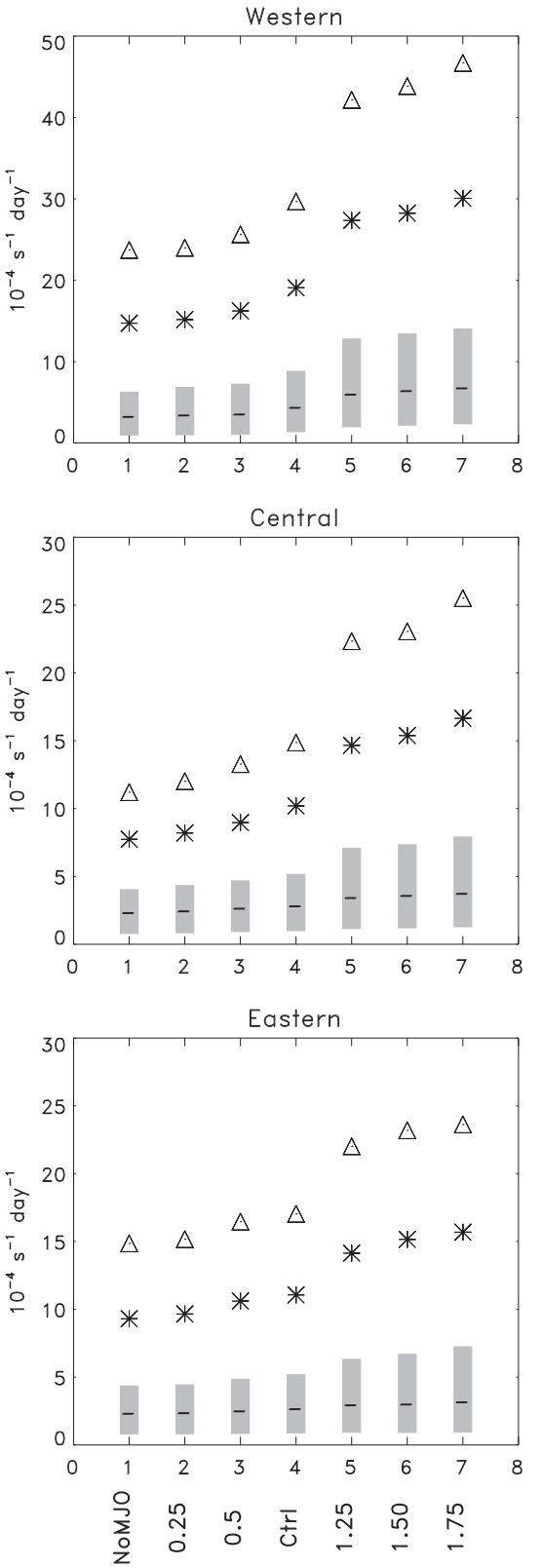

Fig. 16. As in Fig. 12 but for sensitivity of positive absolute vorticity advection at 500-hPa.

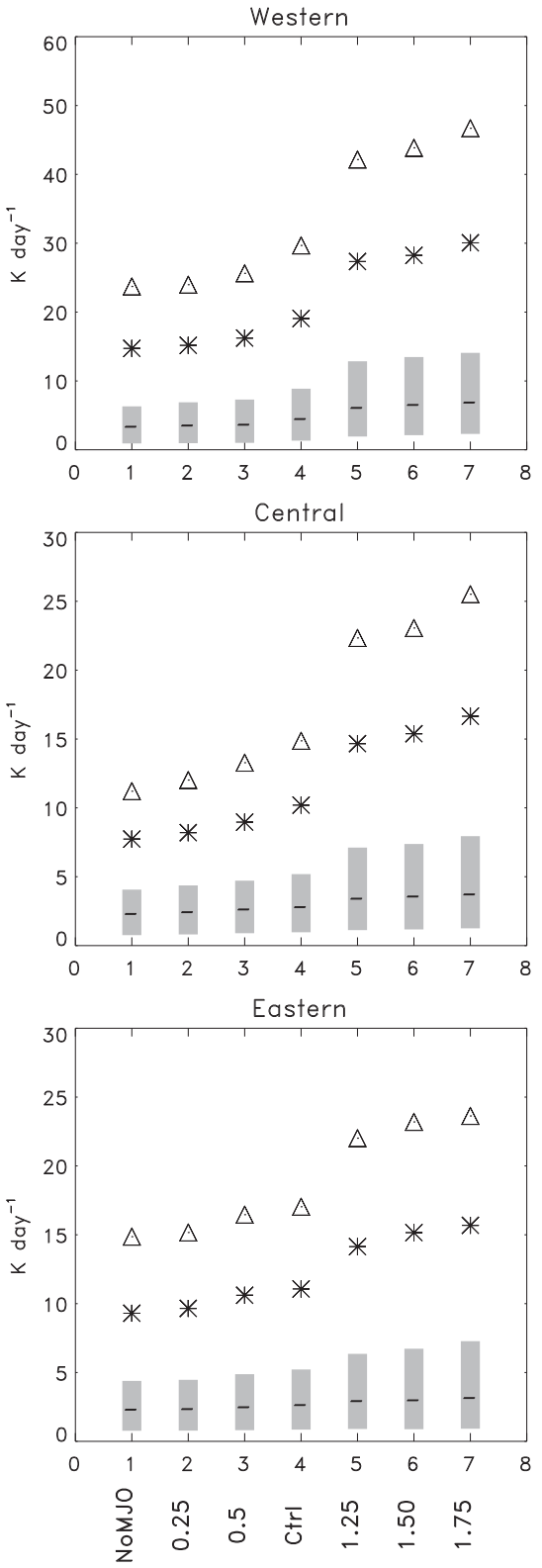

Fig. 17. As in Fig. 12 but for sensitivity of positive advection of temperature at 500-hPa.

MJO, will substantially contribute to monitoring and forecasting hazardous weather events.

Acknowledgments

This research was supported by the Climate and Large-scale Scale Dynamics Program from the National Science Foundation (AGS-1053294). CFSR reanalysis was provided by Research Data Archive at the National Center for Atmospheric Research, Computational and Information Systems Laboratory, Boulder, CO. [Available online at http://rda.ucar.edu/datasets/ds093.0.] The research also benefitted from computational support provide by the CISL, NCAR. OLR data were provided by the NOAA/OAR/ESRL PSD, Boulder, Colorado, USA (www.esrl.noaa.gov) and the gridded precipitation by the Climate Prediction Center (NCEP). The authors would like to thank Jimmy Dudhia for hosting their visit at NCAR and help with some aspects of the WRF model.

References

Barlow, M., Wheeler, M., Lyon, B., Cullen, H., 2005. Modulation of daily precipitation over Southwest Asia by the Madden–Julian Oscillation. Mon. Weather Rev. 133, 3579–3594.
Barry, R.G., Carleton, A.M., 2001. Synoptic and Dynamic Climatology, Routledge (620 pp.).
Becker, E.J., Berbery, E.H., Higgins, R.W., 2011. Modulation of cold-season U.S. daily precipitation by the Madden–Julian Oscillation. J. Clim. 24, 5157–5166.
Bond, N.A., Vecchi, G.A., 2003. The influence of the Madden–Julian Oscillation on precipitation in Oregon and Washington. Weather Forecast. 18, 600–613.
Caldwell, P., 2010. California wintertime precipitation bias in regional and global climate models. J. Appl. Meteorol. Climatol. 49, 2147–2158.
Carvalho, L.M.V., Jones, C., Liebmann, B., 2002. Extreme precipitation events in southeastern South America and large-scale convective patterns in the South Atlantic convergence zone. J. Clim. 15, 2377–2394.
Carvalho, L.M.V., Jones, C., Liebmann, B., 2004. The South Atlantic convergence zone: intensity, form, persistence, and relationships with intraseasonal to interannual activity and extreme rainfall. J. Clim. 17, 88–108.
Cassou, C., 2008. Intraseasonal interaction between the Madden–Julian Oscillation and the North Atlantic Oscillation. Nature 455, 523–527.
Cavazos, T., Rivas, D., 2004. Variability of extreme precipitation events in Tijuana, Mexico. Clim. Res. 25, 229–242.
Changnon, S.D., 2003. Measures of economic impacts of weather extremes. Bull. Am. Meteorol. Soc. 84, 1231–1235.
Changnon, S., 2011. Temporal distribution of weather catastrophes in the USA. Clim. Chang. 106, 129–140.
Changnon, S.A., Pielke Jr., R.A., Changnon, D., Sylves, R.T., Pulwarty, R., 2000. Human factors explain the increased losses from weather and climate extremes. Bull. Am. Meteorol. Soc. 81, 437–442.
Chen, F., Dudhia, J., 2001. Coupling an advanced land surface-hydrology model with the Penn State-NCAR MM5 modeling system. Part I: model implementation and sensitivity. Mon. Weather Rev. 129, 569–585.
Chen, M.Y., Shi, W., Xie, P.P., Silva, V.B.S., Kousky, V.E., Higgins, R.W., Janowiak, J.E., 2008. Assessing objective techniques for gauge-based analyses of global daily precipitation. J. Geophys. Res.-Atmos. 113 (D04110), 04111–04113.
Coleman, R.F., Drake, J.F., McAtee, M.D., Belsma, L.O., 2010. Anthropogenic moisture effects on WRF summertime surface temperature and mixing ratio forecast skill in Southern California. Weather Forecast. 25, 1522–1535.
De Souza, E.B., Ambrizzi, T., 2006. Modulation of the intraseasonal rainfall over tropical brazil by the Madden–Julian Oscillation. Int. J. Climatol. 26, 1759–1776.
Donald, A., et al., 2006. Near-global impact of the Madden–Julian Oscillation on rainfall. Geophys. Res. Lett. 33.
Easterling, D.R., Evans, J.L., Groisman, P.Y., Karl, T.R., Kunkel, K.E., Ambenje, P., 2000a. Observed variability and trends in extreme climate events: a brief review. Bull. Am. Meteorol. Soc. 81, 417–425.
Easterling, D.R., Meehl, G.A., Parmesan, C., Changnon, S.A., Karl, T.R., Mearns, L.O., 2000b. Climate extremes: observations, modeling, and impacts. Science 289, 2068–2074.
Eichler, T., Higgins, W., 2006. Climatology and ENSO-related variability of North American extratropical cyclone activity. J. Clim. 19, 2076–2093.

Gershunov, A., 1998. ENSO influence on intraseasonal extreme rainfall and temperature frequencies in the contiguous United States: implications for long-range predictability. J. Clim. 11, 3192–3203.
Gershunov, A., Barnett, T.P., 1998. ENSO influence on intraseasonal extreme rainfall and temperature frequencies in the contiguous United States: observations and model results. J. Clim. 11, 1575–1586.
Gonzalez, P.L.M., Vera, C.S., Liebmann, B., Kiladis, G., 2008. Intraseasonal variability in subtropical South America as depicted by precipitation data. Clim. Dyn. 30, 727–744.
Gottschalck, J., et al., 2010. A framework for assessing operational Madden–Julian Oscillation forecasts a Clivar MJO Working Group Project. Bull. Am. Meteorol. Soc. 91, 1247–1258.
Grise, K.M., Son, S.W., Gyakum, J.R., 2013. Intraseasonal and interannual variability in North American storm tracks and its relationship to equatorial Pacific variability. Mon. Weather Rev. 141, 3610–3625.
Guan, B., Waliser, D.E., Molotch, N.P., Fetzer, E.J., Neiman, P.J., 2012. Does the Madden–Julian Oscillation influence wintertime atmospheric rivers and snowpack in the Sierra Nevada? Mon. Weather Rev. 140, 325–342.
Gustafson, W.I., Weare, B.C., 2004. MM5 modeling of the Madden–Julian Oscillation in the Indian and west Pacific Oceans: model description and control run results. J. Clim. 17, 1320–1337.
Hendon, H.H., Salby, M.L., 1994. The life-cycle of the Madden–Julian Oscillation. J. Atmos. Sci. 51, 2225–2237.
Hidayat, R., Kizu, S., 2010. Influence of the Madden–Julian Oscillation on Indonesian rainfall variability in austral summer. Int. J. Climatol. 30, 1816–1825.
Higgins, R.W., Schemm, J.K.E., Shi, W., Leetmaa, A., 2000a. Extreme precipitation events in the western United States related to tropical forcing. J. Clim. 13, 793–820.
Higgins, R.W., Shi, W., Yarosh, E., Joyce, R., 2000b. Improved United States precipitation quality control system and analysis. NCEP/Climate Prediction Center ATLAS, No. 7. National Oceanic and Atmospheric Administration (40 pp.).
Higgins, R.W., Silva, V.B.S., Kousky, V.E., Shi, W., 2008. Comparison of daily precipitation statistics for the United States in observations and in the NCEP Climate Forecast System. J. Clim. 21, 5993–6014.
Hirons, L.C., Inness, P., Vitart, F., Bechtold, P., 2013. Understanding advances in the simulation of intraseasonal variability in the ECMWF model. Part I: the representation of the MJO. Q. J. R. Meteorol. Soc. 139, 1417–1426.
Hong, S.Y., Dudhia, J., Chen, S.H., 2004. A revised approach to ice microphysical processes for the bulk parameterization of clouds and precipitation. Mon. Weather Rev. 132, 103–120.
Hong, S.-Y., Noh, Y., Dudhia, J., 2006. A new vertical diffusion package with an explicit treatment of entrainment processes. Mon. Weather Rev. 134, 2318–2341.
Houze, R.A., 2012. Orographic effects on precipitating clouds. Rev. Geophys. 50, RG1001.
Iacono, M.J., Delamere, J.S., Mlawer, E.J., Shephard, M.W., Clough, S.A., Collins, W.D., 2008. Radiative forcing by long-lived greenhouse gases: calculations with the AER radiative transfer models. J. Geophys. Res.-Atmos. 113.
Ikeda, K., et al., 2010. Simulation of seasonal snowfall over Colorado. Atmos. Res. 97, 462–477.
Jankov, I., Bao, J.W., Neiman, P.J., Schultz, P.J., Yuan, H.L., White, A.B., 2009. Evaluation and comparison of microphysical algorithms in ARW-WRF model simulations of atmospheric river events affecting the California coast. J. Hydrometeorol. 10, 847–870.
Jankov, I., et al., 2011. An evaluation of five ARW-WRF microphysics schemes using synthetic GOES imagery for an atmospheric river event affecting the California coast. J. Hydrometeorol. 12, 618–633.
Jeong, J.H., Ho, C.H., Kim, B.M., Kwon, W.T., 2005. Influence of the Madden–Julian Oscillation on wintertime surface air temperature and cold surges in east Asia. J. Geophys. Res.-Atmos. 110. http://dx.doi.org/10.1029/2004JD005408.
Jeong, J.H., Kim, B.M., Ho, C.H., Noh, Y.H., 2008. Systematic variation in wintertime precipitation in East Asia by MJO-induced extratropical vertical motion. J. Clim. 21, 788–801.
Jones, C., 2000. Occurrence of extreme precipitation events in California and relationships with the Madden–Julian Oscillation. J. Clim. 13, 3576–3587.
Jones, C., 2009. A homogeneous stochastic model of the Madden–Julian Oscillation. J. Clim. 22, 3270–3288.
Jones, C., Carvalho, L.M.V., 2006. Changes in the activity of the Madden–Julian Oscillation during 1958–2004. J. Clim. 19, 6353–6370.
Jones, C., Carvalho, L.M.V., 2011. Stochastic simulations of the Madden–Julian Oscillation activity. Clim. Dyn. 36, 229–246 (DOI 210.1007/s00382-00009-00660-00382).
Jones, C., Carvalho, L.M.V., 2012. Spatial-intensity variations in extreme precipitation in the contiguous United States and the Madden–Julian Oscillation. J. Clim. 25, 4898–4913.
Jones, C., Waliser, D.E., Lau, K.M., Stern, W., 2004a. The Madden–Julian Oscillation and its impact on Northern Hemisphere weather predictability. Mon. Weather Rev. 132, 1462–1471.
Jones, C., Waliser, D.E., Lau, K.M., Stern, W., 2004b. Global occurrences of extreme precipitation and the Madden–Julian Oscillation: observations and predictability. J. Clim. 17, 4575–4589.
Jones, C., Gottschalck, J., Carvalho, L.M.V., Higgins, W.R., 2011a. Influence of the Madden–Julian Oscillation on forecasts of extreme precipitation in the contiguous United States. Mon. Weather Rev. 139, 332–350.
Jones, C., Carvalho, L.M.V., Gottschalck, J., Higgins, W.R., 2011b. The Madden–Julian Oscillation and the relative value of deterministic forecasts of extreme precipitation in the contiguous United States. J. Clim. 24, 2421–2428.
Kain, J.S., 2004. The Kain–Fritsch convective parameterization: an update. J. Appl. Meteorol. 43, 170–181.
Kim, J., Waliser, D.E., Neiman, P.J., Guan, B., Ryoo, J.M., Wick, G.A., 2013. Effects of atmospheric river landfalls on the cold season precipitation in California. Clim. Dyn. 40, 465–474.
Kingsmill, D.E., Neiman, P.J., Moore, B.J., Hughes, M., Yuter, S.E., Ralph, F.M., 2013. Kinematic and thermodynamic structures of sierra barrier jets and overrunning atmospheric rivers during a landfalling winter storm in northern California. Mon. Weather Rev. 141, 2015–2036.
Kunkel, K.E., et al., 2013. Monitoring and understanding trends in extreme storms state of knowledge. Bull. Am. Meteorol. Soc. 94, 499–514.
Lalaurette, F., 2003. Early detection of abnormal weather conditions using a probabilistic extreme forecast index. Q. J. R. Meteorol. Soc. 129, 3037–3057.
Lau, W.K.M., Waliser, D.E., 2012. Intraseasonal Variability in the Atmosphere–Ocean Climate System, 2nd edition. , Springer, Chichester, UK (613 pp.).
Lavers, D.A., Villarini, G., 2013. The nexus between atmospheric rivers and extreme precipitation across Europe. Geophys. Res. Lett. 40, 3259–3264.
Legg, T.P., Mylne, K.R., 2004. Early warnings of severe weather from ensemble forecast information. Weather Forecast. 19, 891–906.
L'Heureux, M.L., Higgins, R.W., 2008. Boreal winter links between the Madden–Julian Oscillation and the Arctic Oscillation. J. Clim. 21, 3040–3050.
Liebmann, B., Smith, C.A., 1996. Description of a complete (interpolated) outgoing longwave radiation dataset. Bull. Am. Meteorol. Soc. 77, 1275–1277.
Liebmann, B., Kiladis, G.N., Vera, C.S., Saulo, A.C., Carvalho, L.M.V., 2004. Subseasonal variations of rainfall in South America in the vicinity of the low-level jet east of the Andes and comparison to those in the South Atlantic convergence zone. J. Clim. 17, 3829–3842.
Lin, H., Brunet, G., Derome, J., 2009. An observed connection between the North Atlantic Oscillation and the Madden–Julian Oscillation. J. Clim. 22, 364–380.
Lin, H., Brunet, G., Mo, R., 2010. Impact of the Madden–Julian Oscillation on wintertime precipitation in Canada. Mon. Weather Rev. 138, 3822–3839.
Liu, C.H., Ikeda, K., Thompson, G., Rasmussen, R., Dudhia, J., 2011. High-resolution simulations of wintertime precipitation in the Colorado headwaters region: sensitivity to physics parameterizations. Mon. Weather Rev. 139, 3533–3553.
Long, D., Scanlon, B.R., Fernando, D.N., Meng, L., Quiring, S.M., 2012. Are temperature and precipitation extremes increasing over the U.S. high plains? Earth Interact. 16.
Madden, R.A., Julian, P.R., 1994. Observations of the 40–50-day tropical oscillation—a review. Mon. Weather Rev. 122, 814–837.
Martin, E.R., Schumacher, C., 2010. Modulation of Caribbean precipitation by the Madden–Julian Oscillation. J. Clim. 24, 813–824.
Matthews, A.J., 2000. Propagation mechanisms for the Madden–Julian Oscillation. Q. J. R. Meteorol. Soc. 126, 2637–2651.
Matthews, A.J., 2008. Primary and successive events in the Madden–Julian Oscillation. Q. J. R. Meteorol. Soc. http://dx.doi.org/10.1002/qj.1224.
Matthews, A.J., Hoskins, B.J., Masutani, M., 2004. The global response to tropical heating in the Madden–Julian Oscillation during the northern winter. Q. J. R. Meteorol. Soc. 130, 1991–2011.
Meehl, G.A., et al., 2000. An introduction to trends in extreme weather and climate events: observations, socioeconomic impacts, terrestrial ecological impacts, and model projections. Bull. Am. Meteorol. Soc. 81, 413–416.
Mo, K.C., 1999. Alternating wet and dry episodes over California and intraseasonal oscillations. Mon. Weather Rev. 127, 2759–2776.
Mo, K.C., Higgins, R.W., 1998a. Tropical convection and precipitation regimes in the western United States. J. Clim. 11, 2404–2423.
Mo, K.C., Higgins, R.W., 1998b. Tropical influences on California precipitation. J. Clim. 11, 412–430.
Murakami, M., 1979. Large-scale aspects of deep convective activity over the GATE area. Mon. Weather Rev. 107, 994–1013.
Nogues-Paegle, J., Byerle, L.A., Mo, K.C., 2000. Intraseasonal modulation of South American summer precipitation. Mon. Weather Rev. 128, 837–850.
Palmer, T.N., Hagedorn, R. (Eds.), 2006. Predictability of Weather and Climate. Cambridge University Press, New York (702 pp.).
Pielke Jr., R.A., Downton, M.W., 2000. Precipitation and damaging floods: trends in the United States, 1932–97. J. Clim. 13, 3625–3637.

Pohl, B., Camberlin, P., 2006a. Influence of the Madden–Julian Oscillation on East African rainfall. I: intraseasonal variability and regional dependency. Q. J. R. Meteorol. Soc. 132, 2521–2539.
Pohl, B., Camberlin, P., 2006b. Influence of the Madden–Julian Oscillation on East African rainfall: II. March–May season extremes and interannual variability. Q. J. R. Meteorol. Soc. 132, 2541–2558.
Pohl, B., Matthews, A.J., 2007. Observed changes in the lifetime and amplitude of the Madden–Julian Oscillation associated with interannual ENSO sea surface temperature anomalies. J. Clim. 20, 2659–2674.
Pohl, B., Richard, Y., Fauchereau, N., 2007. Influence of the Madden–Julian Oscillation on Southern African summer rainfall. J. Clim. 20, 4227–4242.
Ralph, F.M., Dettinger, M.D., 2012. Historical and national perspectives on extreme West Coast precipitation associated with atmospheric rivers during December 2010. Bull. Am. Meteorol. Soc. 93, 783–790.
Ralph, F.M., Neiman, P.J., Kiladis, G.N., Weickmann, K., Reynolds, D.W., 2011. A multiscale observational case study of a Pacific atmospheric river exhibiting tropical–extratropical connections and a mesoscale frontal wave. Mon. Weather Rev. 139, 1169–1189.
Rutz, J.J., Steenburgh, W.J., 2012. Quantifying the role of atmospheric rivers in the interior western United States. Atmos. Sci. Lett. 13, 257–261.
Saha, S., et al., 2010. The NCEP climate forecast system reanalysis. Bull. Am. Meteorol. Soc. 91, 1015–1057.
Seo, K.H., Son, S.W., 2012. The global atmospheric circulation response to tropical diabatic heating associated with the Madden–Julian Oscillation during Northern Winter. J. Atmos. Sci. 69, 79–96.
Skamarock, W.C., et al., 2008. A Description of the Advanced Research WRF Version 3 (NCAR/TN-475 + STR, NCAR TECHNICAL NOTE 113 pp.).
Smith, B.L., Yuter, S.E., Neiman, P.J., Kingsmill, D.E., 2010. Water vapor fluxes and orographic precipitation over northern California associated with a landfalling atmospheric river. Mon. Weather Rev. 138, 74–100.
Stein, U., Alpert, P., 1993. Factor separation in numerical simulations. J. Atmos. Sci. 50, 2107–2115.
Thompson, D.W.J., Wallace, J.M., 1998. The Arctic Oscillation signature in the wintertime geopotential height and temperature fields. Geophys. Res. Lett. 25, 1297–1300.
Tribbia, J.J., 1997. Weather prediction. In: Katz, R.W., Murphy, A.H. (Eds.), Economic Value of Weather and Climate Forecasts. Oxford University Press (222 pp.).
Vitart, F., Jung, T., 2010. Impact of the Northern Hemisphere extratropics on the skill in predicting the Madden Julian Oscillation. Geophys. Res. Lett. 37.
Waliser, D.E., Lau, K.M., Stern, W., Jones, C., 2003. Potential predictability of the Madden–Julian Oscillation. Bull. Am. Meteorol. Soc. 84, 33–50.
Weaver, S.J., Wang, W.Q., Chen, M.Y., Kumar, A., 2011. Representation of MJO variability in the NCEP Climate Forecast System. J. Clim. 24, 4676–4694.
Wettstein, J.J., Mearns, L.O., 2002. The influence of the North Atlantic–Arctic Oscillation on mean, variance, and extremes of temperature in the northeastern United States and Canada. J. Clim. 15, 3586–3600.
Wheeler, M.C., Hendon, H.H., 2004. An all-season real-time multivariate MJO index: development of an index for monitoring and prediction. Mon. Weather Rev. 132, 1917–1932.
Wheeler, M.C., Hendon, H.H., Cleland, S., Meinke, H., Donald, A., 2009. Impacts of the Madden–Julian Oscillation on Australian rainfall and circulation. J. Clim. 22, 1482–1498.
Wilks, D.S., 2006. Second edition. Statistical Methods in the Atmospheric Sciences, vol. 91. Academic Press, Inc., San Diego, California, USA (648 pp.).
Zhang, C.D., 2005. Madden–Julian Oscillation. Rev. Geophys. 43, 1–36.
Zhang, C., 2013. Madden–Julian Oscillation: Bridging Weather and Climate. Bull. Am. Meteorol. Soc. 94, 1849–1870.
Zhang, L., Wang, B., Zeng, Q., 2009. Impact of the Madden–Julian Oscillation on summer rainfall in Southeast China. J. Clim. 22, 201–216.
Zhou, S., L'Heureux, M., Weaver, S., Kumar, A., 2011. A composite study of the MJO influence on the surface air temperature and precipitation over the Continental United States. Clim. Dyn. 1–13.
Zhou, S.T., L'Heureux, M., Weaver, S., Kumar, A., 2012. A composite study of the MJO influence on the surface air temperature and precipitation over the Continental United States. Clim. Dyn. 38, 1459–1471.
Zhu, Y., Toth, Z., 2001. Extreme weather events and their probabilistic prediction by the NCEP ensemble forecast system. Preprints of the Symposium on Precipitation Extremes: Prediction, Impact, and Responses (14–19 January 2001, Albuquerque, NM).